Biofilm 4 (2022) 100067

Contents lists available at ScienceDirect

Biofilm

journal homepage: www.sciencedirect.com/journal/biofilm

Competitive advantage of oral streptococci for colonization of the middle ear mucosa

Kristin M. Jacob, Gemma Reguera *

Department of Microbiology and Molecular Genetics, Michigan State University, East Lansing, MI, USA

ARTICLE INFO

Keywords:
Middle ear
Eustachian tube
Biofilms
Otic microbiome
Oral cavity
Otopathogen
Mucin

ABSTRACT

The identification of a diverse microbiome in otic secretions from healthy young adults challenged the entrenched dogma of middle ear sterility and underscored previously unknown roles for oral commensals in the seeding of otic biofilms. We gained insights into the selective forces that enrich for specific groups of oral migrants in the middle ear mucosa by investigating the phylogeny and physiology of 19 strains isolated previously from otic secretions and representing otic commensals (*Streptococcus*) or transient migrants (*Staphylococcus, Neisseria* and actinobacterial *Micrococcus* and *Corynebacterium*). Phylogenetic analyses of full length 16S rRNA sequences recovered from partially sequenced genomes resolved close relationships between the isolates and (peri)oral commensals. Physiological functions that facilitate mucosal colonization (swarming motility, surfactant production) and nutrition (mucin and protein degradation) were also widespread among the cultivars, as was their ability to grow in the presence or absence of oxygen. Yet, streptococci stood out for their enhanced biofilm-forming abilities under oxic and anoxic conditions and ability to ferment host-derived mucosal substrates into lactate, a key metabolic intermediate in the otic trophic webs. Additionally, the otic streptococci inhibited the growth of common otopathogens, an antagonistic interaction that could exclude competitors and protect the middle ear mucosa from infections. These adaptive traits allow streptococcal migrants to colonize the otic mucosa and grow microcolonies with syntrophic anaerobic partners, establishing trophic interactions with other commensals that mirror those formed by the oral ancestors in buccal biofilms.

1. Introduction

The oral cavity provides a heterogenous landscape of surfaces and microenvironments (teeth, gingiva, tongue, cheek, hard and soft palate, etc.) for diverse microbial communities [16]. The availability of dietary substrates supports the growth and diversification of oral commensals and makes these communities some of the richest and most diverse in the human body [79]. Many of these microbes readily disperse via saliva and saliva aerosols into perioral regions [16] and, from there, to other parts of the aerodigestive tract [23]. The saliva aerosols also enter the middle ear through the tubal extension of the tympanic cavity (the tympanic or Eustachian tube, Fig. 1) [6]. The tube is passively collapsed at rest to sound proof the tympanic cavity and minimize microbial entry, yet it opens when we swallow or yawn to draw in air from the lower airways (Fig. 1) [6]. The cycles of aperture and collapse of the Eustachian tube promote the intermittent aeration of the tympanic cavity, relieve negative pressure across the eardrum and drain into the nasopharynx excess mucus and fluids [6].

The episodic ventilation of the middle ear reduces oxygen availability to the otic mucosa and establishes redox conditions that favor the growth of anaerobes [44]. In support of this, strictly anaerobic genera in the Bacteroidetes (*Prevotella* and *Alloprevotella*), Fusobacteria (*Fusobacterium* and *Leptotrichia*) and Firmicutes (*Veillonella*) are more abundant in otic secretions collected at the nasopharyngeal orifice of the Eustachian tube than in oral samples [44]. The genus *Streptococcus*, which includes mostly facultative anaerobes [54], is also enriched in otic secretions [44]. The co-enrichment of streptococci with Bacteroidetes and *Veillonella* spp. in otic secretions suggests that these groups are part of syntrophic consortia (Fig. 1) similar to those described in oral biofilms [44]. This model (Fig. 1) is based on the metabolic co-dependency of Bacteroidetes to break down mucin glycoproteins and other mucosal proteins into sugars and peptides, which some streptococci ferment into lactate [33] to sustain propionate and acetate production by *Veillonella* [12,15]. The lactate dependency of *Veillonella* spp. may also favor direct metabolic interactions with lactate-producing Bacteroidetes partners [62]. Through their collective activities,

* Corresponding author. 567 Wilson Rd., Rm, 6190 Biomedical & Physical Sciences building East Lansing, MI, 48824, USA.
E-mail address: reguera@msu.edu (G. Reguera).

https://doi.org/10.1016/j.biofilm.2022.100067
Received 30 August 2021; Received in revised form 17 December 2021; Accepted 10 January 2022
Available online 18 January 2022

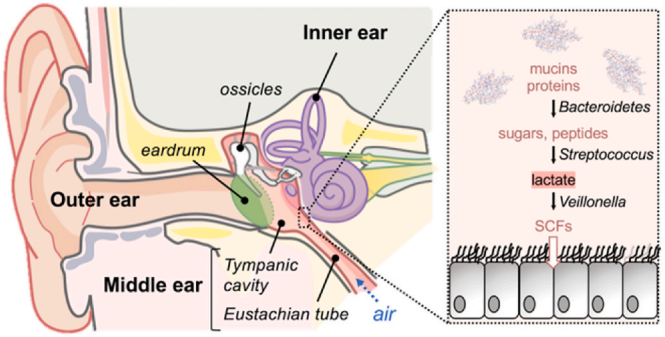

Fig. 1. Illustration of the human ear anatomy (*left*) and trophic webs within bacterial microcolonies in the middle ear mucosa (*right*). The human ear is divided in three compartments (outer, middle, and inner). The eardrum separates the outer ear canal from the tympanic cavity of the middle ear, which extends as a tube (tympanic or Eustachian tube) into the nasopharynx to draw in air and drain otic secretions. The microbiome sequenced from otic secretions of healthy young adults [44] supports the establishment of a trophic web (inset) for the degradation of host mucins and proteins by Bacteroidetes into substrates (sugars and peptides) that *Streptococcus* and *Veillonella* cooperatively ferment into short chain fatty acids (SCFs) via lactate.

Bacteroidetes, streptococci and *Veillonella* are predicted to degrade and ferment host-derived nutrients (mucins and proteins) into short chain fatty acids known to contribute to mucosal health in other body sites [5].

Although oral-like consortia are predicted to colonize the middle ear in health [44], the physiological traits that facilitate mucosal colonization remain largely unknown. The presence of bacterial microcolonies in biopsy specimens of the mucosal lining of the tympanic cavity [28,71] points at biofilm formation as a critical selective factor for the growth of otic commensals. Microcolonies protect mucosal colonizers against immunoattack and clearance [68]. The latter is particularly vigorous closer and within the Eustachian tube, due to the higher density of cilial cells in these regions and the pumping force exerted by the periodic contraction and relaxation of muscles around the Eustachian tube (muscular clearance) [29,63]. Additionally, microcolonies protect anaerobic commensals from oxygen intrusions when the Eustachian tube opens [6]. The aggregative nature of many oral streptococci is expected to facilitate firm attachment of colonizers to the otic epithelium and the formation of microcolonies with anoxic niches for anaerobic syntrophic partners [39]. To test this, we investigated the colonization potential of streptococcal commensals and transient migrants (*Staphylococcus, Neisseria* and actinobacterial *Micrococcus* and *Corynebacterium*) previously recovered from otic secretions [44]. Streptococcal and staphylococcal species are, for example, among the most prominent members in the oral and nasal microbiomes, respectively [8,23]. Both groups disperse in the aerodigestive tract and enter the middle ear during the intermittent openings of the Eustachian tube. Yet, while streptococci are abundant in otic secretions from healthy individuals, staphylococcal-like sequences are seldom detected [44]. This suggests that streptococcal migrants have a competitive advantage over the transient staphylococcal species during the colonization of the middle ear mucosa. Hence, we sequenced and partially assembled the genomes of otic streptococcal and non-streptococcal cultivars (19 in all) [44] and used the full length 16S rRNA sequences to identify their closest relatives. We then screened the cultivars for adaptive traits predicted to be important for mucosal colonization (e.g., motility in mucus, microcolony formation) and for growth under conditions (redox, nutritional) relevant to the middle ear microenvironment. Our study revealed similar adaptive traits for mucosal growth by the isolates but aggregative and metabolic properties of streptococci critical for successful colonization of the middle ear mucosa. These same properties are retained from their closest oral ancestors, with whom they share the ability to establish trophic webs with anaerobes and antagonize competitors. These findings provide novel insights into the adaptive responses that sustain the growth and functionality of otic communities and could influence the outcome of infections.

2. Results

2.1. Phylogenetic analysis supports the oral ancestry of otic streptococcal commensals

A previous study of the microbiology of the middle ear [44] recovered from healthy young adults 19 cultivars representing otic *Streptococcus* commensals and transient or low abundant groups (*Staphylococcus, Neisseria,* and the actinobacterial genera *Micrococcus* and *Corynebacterium*). Phylogenetic analysis of partial 16S rDNA amplicons sequenced from the isolates revealed close relationships with oral (oropharyngeal and buccal) strains recovered from the same hosts [44]. To reach the resolution needed for species-level demarcation, we sequenced and partially assembled the genomes of the otic cultivars and retrieved full-length 16S rRNA sequences for each of the isolates. A species sequence identity cutoff of >98.7% [70] matched each otic isolate to more than one species within each genus (Table 1 shows the top identity hit for each strain). Phylogenetic inference methods

Table 1
Taxonomic classification (reference strain) of otic strains based on the % identity (ID) of their full-length 16S rRNA sequence.

Strain	GenBank no.	Reference Strain (Accession; % ID)
Streptococcus		
L0020-02	MW866489	*Streptococcus parasanguinis* (NR_024842.1; 99.47)
L0021-01	MW866494	*Streptococcus salivarius* (NR_042776.1; 99.81)
L0021-04	MW866496	*Streptococcus salivarius* (NR_042776.1; 99.81)
L0021-05	MW866497	*Streptococcus salivarius* (NR_042776.1; 99.81)
L0022-03	MW866499	*Streptococcus salivarius* (NR_042776.1; 99.81)
L0022-04	MW866500	*Streptococcus salivarius* (NR_042776.1; 99.81)
L0022-05	MW866501	*Streptococcus salivarius* (NR_042776.1; 99.81)
L0022-06	MW866502	*Streptococcus salivarius* (NR_042776.1; 99.81)
L0023-01	MW866503	*Streptococcus agalactiae* (NR_040821.1; 100)
L0023-02	MW866504	*Streptococcus oralis* (NR_117719.1; 99.47)
L0023-03	MW866505	*Streptococcus agalactiae* (NR_040821.1; 100)
Staphylococcus		
L0020-04	MW866491	*Staphylococcus hominis* (NR_036956.1; 99.61)
L0021-02	MW866495	*Staphylococcus aureus* (NR_037007.2; 99.87)
L0021-06	MW866498	*Staphylococcus saccharolyticus* (NR_113405.1; 99.4)
Micrococcus		
L0020-05	MW866492	*Micrococcus luteus* (NR_075062.2, 99.61)
Corynebacterium		
L0020-06	MW866493	*Corynebacterium pseudodiphtericum* (NR_042137.1; 99.47)
Neisseria		
L0020-03	MW866490	*Neisseria perflava* (NR_114694; 99.93)
L0023-05	MW866507	*Neisseria perflava* (NR_117694.1; 99.74)
L0023-06	MW866506	*Neisseria perflava* (NR_117694.1; 99.74)

resolved, however, close evolutionary ties with oral commensals or species that disperse from perioral regions (Fig. 2).

The nearest neighbor to most of the *Streptococcus* sequences (7 of them) was *Streptococcus salivarius* (subspecies *salivarius* and *thermophilus*) (Fig. 2). Genomic divergence (size and gene content) for species and subspecies within the Salivarius group is high [14]. As a result, strains of *S. salivarius* can have very different metabolic and physiological characteristics or even habitat/host preferences despite sharing high 16S rRNA sequence identity [14,21]. Thus, the physiology of otic and oral strains in the *S. salivarius* subclade may differ substantially. The remaining streptococcal sequences clustered separately with oral relatives within the Mitis group (L0020-02 and *Streptococcus parasanguinis*), Viridans group (L0023-02 and *Streptococcus pseudopneumoniae*) and the Lancefield's group B streptococcus or GBS (L0023–01 and L0023-03 and *Streptococcus agalactiae*) [21,30] (Fig. 2). Hence, 16S rRNA phylogeny supports the oral ancestry of all the streptococcal cultivars [44].

The 16S rRNA sequence identity of the non-streptococcal strains also produced more than one match to species of *Staphylococcus, Neisseria, Micrococcus* and *Corynebacterium* (Table 1). A catalase positive test confirmed the classification of the three staphylococcal isolates as *Staphylococcus* spp. (Fig. 2). The closest neighbors to the otic staphylococci were species (*Staphylococcus hominis, Staphylococcus aureus*, and *Staphylococcus epidermidis*) that are highly represented in the nasal passages [8]. Their nasal abundance facilitates dispersal in the contiguous oral cavity [52] and their transient detection in perioral regions [48,52]. On the other hand, the three *Neisseria* isolates were closely related to oropharyngeal commensals [36,45] (*Neisseria perflava, Neisseria subflava* and *Neisseria flavescens*; Fig. 2) that transiently disperse in the aerodigestive tract and the middle ear [44] via saliva aerosols [2]. The otic isolates also included two actinobacterial *Micrococcus* and *Corynebacterium* strains (Table 1). The *Micrococcus* isolate was catalase-positive, a general phenotypic trait of the genus [37], and branched closely to *Micrococcus yunnanensis* (Fig. 2). This is a soil *Micrococcus* species [84] that, like other environmental micrococci, enters the human aerodigestive tract with air [40]. The second actinobacterial isolate was closely related to *Corynebacterium pseudodiphtericum* (Fig. 2). *Corynebacterium* commensals are prominent members of the nasal microbiomes and antagonists of nasal pathobionts, including some of the most important otopathogens [9]. Their abundance in the nasal microflora explains their detection in oral and perioral regions [41]. However, actinobacteria only account for ~1% of the operational taxonomic units (OTUs) in otic secretions, suggesting they are negatively selected for growth and reproduction in the middle ear mucosa [44].

2.2. Surfactant-mediated swarming motility is widespread among the otic cultivars

Successful colonization of respiratory mucosae requires bacterial migrants to move rapidly across the mucus layer in order to avoid immune attack and clearance [68]. Some flagellated bacteria can reach the underlying epithelial lining by rapidly swarming in groups through the viscous mucoid layer, a process that is stimulated by the lubricating effect of surfactants and mucin glycoproteins [53]. Swarming (flagellated) and swarming-like (non-flagellated) behaviors can be identified in laboratory plate assays that test the expansion of microcolonies on a soft agar (0.4–0.5%) surface [53]. Thus, we tested the ability of the 19 otic isolates to swarm on the surface of 0.5% tryptone soy agar (TSA) plates in reference to the robust swarmer *Pseudomonas aeruginosa* PA01 [38]. Fig. 3A shows the average expansion of triplicate colonies over time

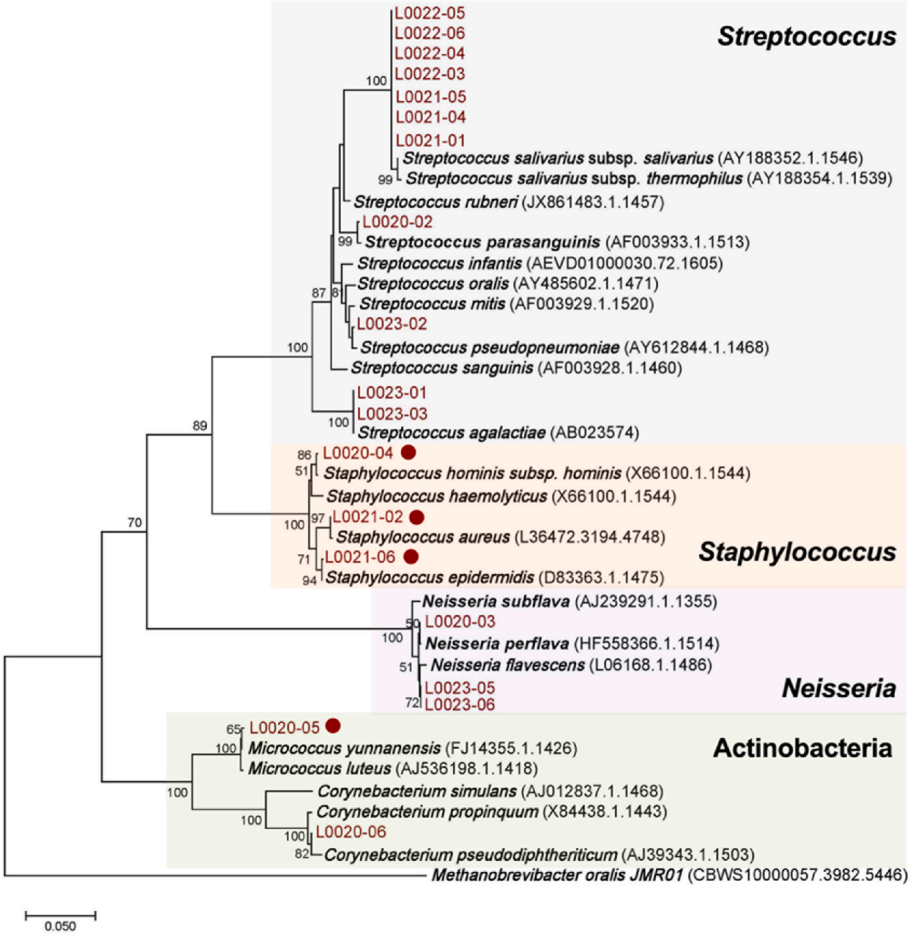

Fig. 2. 16S rRNA gene phylogeny of otic cultivars. Maximum-likelihood tree constructed with full-length 16S rRNA sequences from the otic isolates and the closest reference strains (accession numbers in parentheses). The scale bar indicates 5% sequence divergence filtered to a conservation threshold above 79% using the Living Tree Database [51,83]. Bootstrap probabilities by 1000 replicates at or above 50% are denoted by numbers at each node. The circles identify catalase-positive isolates.

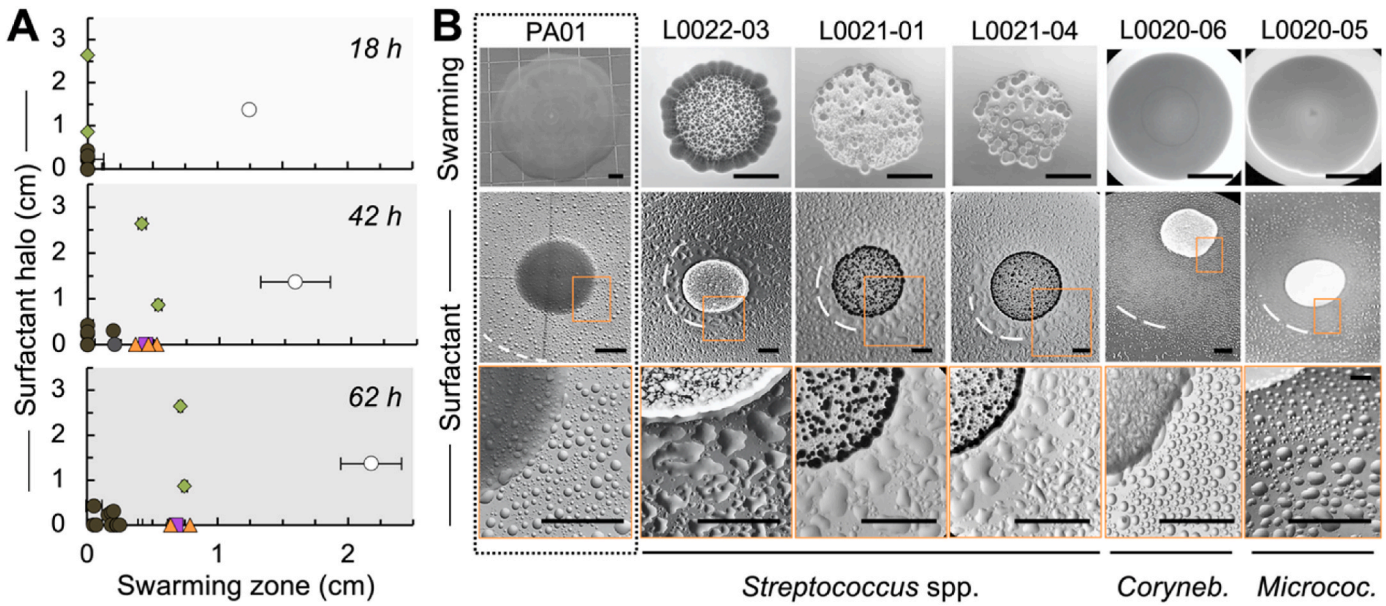

Fig. 3. Swarming motility and surfactant production by otic cultivars in reference to *Pseudomonas aeruginosa* PA01. (A) Average surfactant production (halo of mineral oil dispersal around 24h colonies grown on 1.5% TSA), and size of swarming expansion (0.5% TSA plates at 18, 42 and 62 h) measured in triplicate replicates of the otic isolates (*Streptococcus*, gray circles; *Staphylococcus*, orange triangles; *Neisseria*, purple squares; actinobacterial strains of *Corynebacterium* and *Micrococcus*, green diamonds) and the positive control (*P. aeruginosa* PA01, white circles). **(B)** Representative images of swarming (0.4% TSA, 42 h) and surfactant (1.5% TSA, 24 h) plate assays for *P. aeruginosa* PA01 (positive control, boxed) and otic strains of *Streptococcus, Corynebacterium,* and *Micrococcus* (scale bars, 0.5 cm). The edge of the surfactant halo is highlighted with a dashed white line. The orange box identifies approximate areas of the colony edge and surfactant dispersion zone enlarged in the bottom images. (For interpretation of the references to color in this figure legend, the reader is referred to the Web version of this article.)

Table 2
Coaggregation, swarming motility and surfactant production of otic isolates in reference to positive control (*P. aeruginosa* PA01).

Species/closest relative	Strain	Aggregation[a]	Surfactant[b]	Swarming[c]		
				18 h	42 h	62 h
Streptococcus						
S. parasanguinis	L0020-02	+	–	–	–	0.07 (0.10)
S. salivarius	L0021-01	+	0.23 (0.19)	–	–	0.16 (0.05)
S. salivarius	L0021-04	+	0.46 (0.09)	–	–	0.05 (0.13)
S. salivarius	L0021-05	+	–	–	–	0.05 (0.07)
S. salivarius	L0022-03	+	0.28 (0.19)	–	–	0.19 (0.004)
S. salivarius	L0022-04	+	–	–	–	0.20 (0.08)
S. salivarius	L0022-05	+	0.18 (0.12)	–	–	0.20 (0.03)
S. salivarius	L0022-06	+	0.09 (0.06)	–	–	0.18 (0.02)
S. agalactiae	L0023-01	+	–	–	0.21 (0.02)	0.23 (0.02)
S. pseudopneumoniae	L0023-02	+	–	–	–	0.07 (0.10)
S. agalactiae	L0023-03	+	0.31 (0.11)	–	0.19 (0.01)	0.20 (0.06)
Staphylococcus						
S. hominis	L0020-04	–	–	–	0.37 (0.004)	0.66 (0.08)
S. aureus	L0021-02	–	–	–	0.53 (0.002)	0.79 (0.001)
S. epidermidis	L0021-06	–	–	–	0.46 (0.03)	0.64 (0.02)
Actinobacteria						
M. yunnanensis	L0020-05	–	0.86 (0.13)	–	0.54 (0.05)	0.75 (0.04)
C. pseudodiphtericum	L0020-06	–	2.64 (0.05)	–	0.41 (0.06)	0.72 (0.03)
Neisseria						
N. perflava	L0020-03	–	–	–	0.44 (0.03)	0.68 (0.001)
N. flavescens	L0023-05	+	–	–	–	0.23 (0.32)
N. flavescens	L0023-06	+	–	–	–	0.25 (0.35)
P. aeruginosa	PA01	–	1.37 (0.06)	1.24 (0.35)	1.58 (0.53)	2.18 (0.47)

[a] Aggregative (+) or uniform (–) growth of cultures spotted on 0.5% TSA plates.
[b] Average (and standard deviation) of triplicate surfactant haloes (cm) measured as the zone of mineral oil dispersion around colonies grown at 37°C on 1.5% TSA plates. (–, not detected).
[c] Average (and standard deviation) of triplicate swarming expansion zones (cm) around colonies grown at 37°C on soft agar (0.5%) TSA plates for 18, 42 and 62 h (–, not detected).

(Table 2). Although *P. aeruginosa* showed large zones of swarming expansion already at 18 h, we only detected swarming activity in the otic isolates after 42 or 62 h of colony growth (Fig. 3A). Lag phases are not unusual prior to swarming on agar plates as cells reprogram their physiology to be able to grow on the agar-solidified medium [53]. Consistent with this, the strains that grew faster on the semisolid TSA

plates (three staphylococcal and the two actinobacterial isolates) produced visible zones of swarming expansion at 42 h, while the slowest growers (*N. perflava* (L0023–05 and L0023-06) required 62 h of incubation (Table 2). Notably, most of the streptococci grew well in tryptone soy broth (TSB), yet they aggregated strongly when growing on the surface of the soft-agar plates (Fig. 3B), which delayed swarming (Table 2). We partially rescued the swarming delay by lowering the agar concentration from 0.5 to 0.4% (Fig. 3B). For example, the streptococcal strain L0022-03 did not swarm on 0.5% TSA plates until after 62 h (Table 2) but expanded 0.28 cm away from the edge of the initial colony after 42 h of growth on 0.4% TSA plates (Fig. 3B). This is because lowering the agar concentration facilitates water movement to the surface and immerses the cells in a layer of liquid that reduces frictionally forces between the cell and the surface and stimulates swarming [53].

The need for some bacteria to express cellular components (flagella, exopolysaccharide, surfactants, etc.) mediating swarming on semisolid agar can also delay the appearance of expansion zones [53]. Secretion of surfactants is particularly important to reduce frictional resistance between the surface of swarming cells and the underlying substratum [53]. As a result, the concentration and diffusion rates of secreted surfactants in soft-agar medium often correlate well with the extent of swarming expansion [10]. Therefore, we also screened for surfactant production by colonies grown on hard agar plates (1.5% TSA) for 24 h and air-brushed with a fine mist of mineral oil droplets. This atomized oil assay instantaneously reveals halos of oil droplet dispersal around surfactant-producing strains and provides a semiquantitative estimation of surfactant production, even at concentrations too low to be detected by traditional methods such as the water drop collapse assay [10]. The assay detected haloes of oil dispersal around 9 of the isolates (Table 2) and identified positive correlations between surfactant production and the onset of swarming on 0.5% TSA for most strains (Fig. 3A). For example, the actinobacterial isolates, which were robust swarmers, produced the highest levels of surfactant (Table 2). By contrast, temperate swarmers such as the streptococcal isolates produced low or undetectable levels of surfactants under the experimental conditions. As an exception, the staphylococcal isolates swarmed robustly on the soft agar plates (Fig. 3) although they did not produce detectable halos of mineral oil dispersion (Table 2). Although staphylococcal cells lack flagellar locomotion, they can passively 'spread' on soft agar surfaces [32] through the coordinated synthesis of lubricating peptides known as phenol-soluble modulins (PSMs) [73]. PSM surfactants accumulate very close to the colony edge [56]. Hence, they are unlikely to produce a halo of oil dispersal in the atomized assay used for testing.

2.3. Redox and nutritional advantage of otic streptococci in the middle ear mucosa

Successful colonizers of the middle ear mucosa face sharp redox fluctuations due to the brief (400 ms) yet infrequent (approximately every minute when we swallow) openings of the Eustachian tube [6]. For this reason, we tested the ability of the otic cultivars to grow under aerobic or anaerobic conditions (Fig. 4A). All the isolates grew well in oxic and anoxic liquid medium, except for two *Neisseria* strains (L0023–05 and L0023-06) that grew slowly in the oxic broth. These two strains flocculated extensively in the oxic medium, an aggregative behavior exhibited by microaerophiles in response to elevated (and toxic) concentrations of oxygen [4]. Pairwise comparisons (two-tailed *t*-test) also identified significant differences in the redox preference of most of the streptococcal and staphylococcal strains (Table 3). Despite these differences, the streptococcal and staphylococcal strains grew faster aerobically and anaerobically (0.56 ± 0.23 and 0.50 ± 0.12 doubling times, respectively) than most other strains, suggestive of a competitive advantage for growth and reproduction under sharp redox fluctuations. The actinobacterial strains also grew in the presence or absence of oxygen but showed a more pronounced redox preference (Table 3). For example, both isolates doubled approximately every 0.5 h under anoxic conditions but slower (*Micrococcus* L0020-05, ~0.74 h doubling time) or faster (*Corynebacterium* L0020-06, 0.17 h average generation time) in oxic media (Table 3). The aerobic preference of the *Corynebacterium* L0020-06 strain matches well with the enrichment of this genus in the aerated nasal passages [8] and the reduced abundance of this group in otic secretions [44].

In addition to redox fluctuations, bacteria colonizing the otic mucosa must cope with a scarcity of nutrients. The limited carriage of dietary substrates in saliva aerosols reduces nutrient availability in the middle ear and is predicted to select for commensals that can use host-derived nutrients such as mucosal proteins and mucin glycoproteins to grow [44]. A screening for the secretion of proteases and mucinases by the otic isolates supported this prediction (Table 3). For these experiments, we spot-plated the cultivars onto TSA plates supplemented with 5% lactose-free skim milk (protease assay) or 0.5% porcine gastric mucin (mucinase assay) for 24 h to identify zones of substrate degradation around the colonies. Fig. 4B shows typical results for representative otic strains and the positive control *P. aeruginosa* PA01. All the isolates were

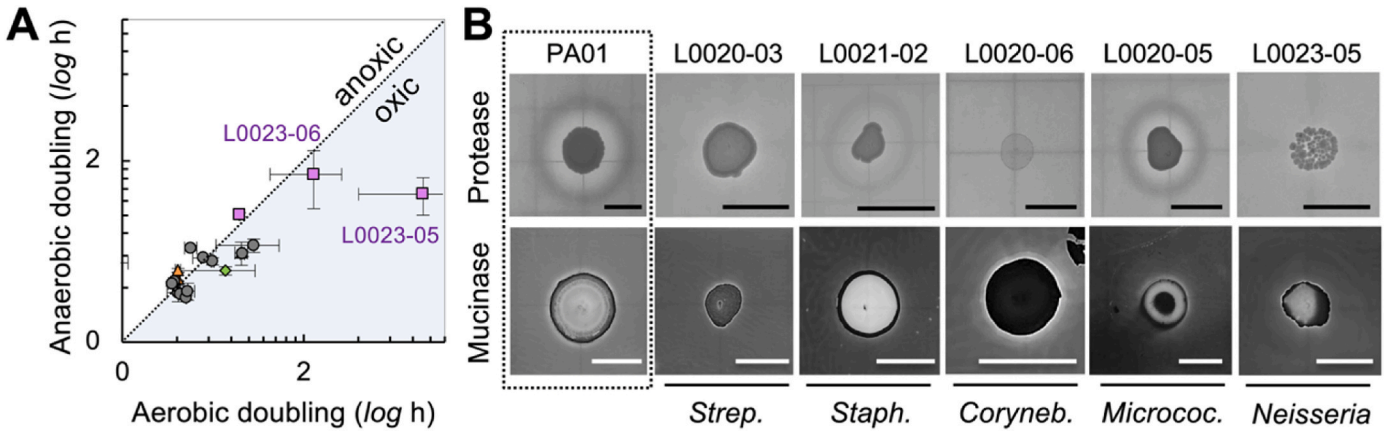

Fig. 4. Growth of otic isolates as a function of oxygen availability and host nutrients (protein and mucin). (A) Average doubling times of otic isolates growing in at least triplicate TSB cultures aerobically or anaerobically at 37°C. Symbols: *Streptococcus* (gray circles), *Staphylococcus* (orange triangles), *Neisseria* (purple squares) and actinobacterial genera *Micrococcus* and *Corynebacterium* (green diamonds). The flocculating strains of *Neisseria* are labeled. The raw data plotted in this graph and significant differences between aerobic and anaerobic generations times for each strain are shown in Table 3. **(B)** Protease and mucinase activity (haloes of milk casein or porcine gastric mucin degradation, respectively) of representative otic isolates and *P. aeruginosa* PA01 (positive control, boxed). The milk casein plates were photographed without staining after 24 h of incubation at 37°C. The mucin plates were incubated for 48 h and stained with 0.1% amido black prior to photography. Scale bars, 0.5 cm. (For interpretation of the references to color in this figure legend, the reader is referred to the Web version of this article.)

Table 3
Growth (aerobic and anaerobic doubling times) and extracellular enzymatic activity (protease and mucinase) of otic isolates. Doubling times are in hours (standard deviation of triplicate cultures in parenthesis; nt, not tested). Protease and mucinase activities were determined by the presence (+) or absence (−) of a halo of degradation in TSA plates supplemented with skim milk (protease assay) or mucin (mucinase assay) after 24 h of growth in reference to a positive control (*P. aeruginosa* PA01). The presence of a faint halo is indicated with "+/−".

		Doubling time (h)[a]		Extracellular enzymes	
Species/closest relative	Strain	Aerobic	Anaerobic	Protease	Mucinase
Streptococcus					
S. parasanguinis	L0020-02	0.629 (0.011)	0.558 (0.026)*	−	+
S. salivarius	L0021-01	0.389 (0.008)**	0.431 (0.006)	−	+/−
S. salivarius	L0021-04	0.376 (0.018)*	0.419 (0.012)	+	+
S. salivarius	L0021-05	0.407 (0.054)	0.375 (0.041)	+	+
S. salivarius	L0022-03	0.419 (0.008)	0.367 (0.004)**	+	+/−
S. salivarius	L0022-04	0.451 (0.003)	0.352 (0.009)**	+	+/−
S. salivarius	L0022-05	0.459 (0.042)	0.381 (0.041)	+	+
S. salivarius	L0022-06	0.487 (0.037)*	0.661 (0.021)	+	+
S. agalactiae	L0023-01	0.561 (0.071)	0.583 (0.009)	+	+
S. pseudopneumoniae	L0023-02	1.026 (0.404)	0.682 (0.058)	−	+
S. agalactiae	L0023-03	0.918 (0.026)	0.614 (0.022)***	+	+
Staphylococcus					
S. hominis	L0020-04	0.907 (0.073)	0.621 (0.091)*	+	+
S. aureus	L0021-02	0.406 (0.006)	0.446 (0.037)	+	+
S. epidermidis	L0021-06	0.406 (0.013)**	0.498 (0.012)	+	+
Actinobacterial species					
M. yunnanensis	L0020-05	1. 048 (0.060)	0.495 (0.026)*	−	+
C. pseudodiphtericum	L0020-06	0.173 (0.042)***	0.546 (0.127)	−	+
Neisseria					
N. perflava	L0020-03	0.885 (0.008)*	1.008 (0.026)	−	+
N. flavescens	L0023-05	9.089 (5.068)	1.307 (0.305)	−	+
N. flavescens	L0023-06	2.273 (0.967)	1.680 (0.593)	−	+
P. aeruginosa	PA01	nt	nt	+	+

[a] Two-tailed *t*-test significance identifying fastest growth conditions (aerobic or anaerobic): $p < 0.05$*, $p < 0.005$**, $p < 0.0005$***.

able to degrade mucin under these conditions, although some strains required additional incubation (48 h) to produce a clear halo (Table 3). As an example of delayed hydrolysis, three aggregative strains of *S. salivarius* (L0021–01, L0022–03 and L0022-04) produced only faint mucin clearings after 24 h (+/− in Table 3) but the zone of degradation expanded after incubating for 48 h. While mucinase activity was widespread, protease activity was only detected in the streptococcal and staphylococcal groups (Table 3). It is unlikely that the casein substrate used in the assays produced false negatives, because extracellular proteases typically have low substrate selectivity and cleave a wide range of substrates [76]. This is particularly advantageous in the middle ear mucosa, where colonizers must scavenge nitrogen sources by breaking downs mucosal proteins and the protein backbone of mucins [60]. In addition to providing a metabolic advantage, proteases facilitate mucosal penetration, control mucus viscosity, modulate host immune responses, and antagonize competitors [35]. Hence, protease secretion confers on staphylococci and streptococci a competitive advantage for otic colonization.

2.4. Metabolic advantage of streptococci for syntrophic growth in biofilms

The presence of bacterial microcolonies on the epithelial surface of biopsy specimens collected from the tympanic cavity of healthy individuals [71] motivated us to investigate the biofilm-forming abilities of the otic isolates. For these assays, we stained 24-h biofilms with crystal violet and measured the absorbance of the biofilm-associated dye to estimate the biofilm biomass (Fig. 5A). All but two streptococcal strains (*S. pseudopneumoniae* L0023-02 and *S. agalactiae* L0023-03) formed robust biofilms under aerobic conditions (Fig. 5A). The group of *S. salivarius* L0021–04 and L0021-05, *S. parasanguinis* L0020-02, and *S. agalactiae* L0023-01 clustered separately with a staphylococcal isolate (*S. aureus* L0021-02) based on their ability to form robust biofilms in both oxic and anoxic media (Fig. 5A). A group comprised of *S. salivarius* L0021–01, L0022–03, L0022–04, L0022–05 and L0022-06 had a biofilm growth advantage in oxic medium only (Fig. 5A). The enhanced biofilm abilities of these isolates correlated well with the pH drops measured in the culture broth at 24 h (Fig. 5B). Indeed, K-means clustering analyses partitioned the best biofilm formers (9 streptococci and *S. aureus* L0021-02 with an average biofilm biomass A_{550}~2.2) separately from all other strains based on the low pH (average pH~4.8) of the medium. The culture pH also partitioned the low biofilm formers (average biofilm biomass $A_{550} \leq 0.1$) in two clusters: one with the two actinobacterial strains (average pH~7.7) and another with the remaining strains (average pH~5.6). Collectively, the clustering of strain phenotypes in three separate groups explained 91.3% of the data variance.

The pH measurements correlated well with lactate levels in the culture broth ($p = 0.03$) and entry in stationary phase (Fig. 5C). Thus, the best biofilm formers produced more lactate than any other strain and entered stationary phase (0.62 ± 0.05 OD_{600}) once the pH dropped below 5. This response is similar to that described for oral streptococcal commensals, which also produce lactic acid as the main fermentation byproduct [69] and stop growing once the pH drops to inhibitory levels, usually at or below 5 [67]. To prevent growth inhibition, commensal oral streptococci co-aggregate with lactate-utilizing bacteria such as *Veillonella* [46]. A similar metabolic dependence via lactate helps explain the co-enrichment of *Streptococcus* and *Veillonella* sequences in otic secretions [44].

2.5. Antagonistic interactions of otic streptococci with common otopathogens

Commensal oral streptococci mediate intra- and interspecies antagonistic interactions in oral biofilms that are critical to dental and mucosal health [39]. Given their oral ancestry, we screened the otic streptococci for their ability to inhibit the growth of known otopathogens (*Streptococcus pneumoniae, Moraxella catarrhalis*, and non-typeable *Haemophilus influenzae*). For these assays, we followed the same protocol as in other plate assays and spot-plated overnight cultures on TSA plates before incubating them at 37°C. After allowing the colonies to grow for 24h, we covered them with a soft (0.75%) agar overlay containing a diluted cell suspension of each otopathogen in a growth medium suitable for their growth. Incubation of the overlayed plates for an additional 24 h revealed clear zones of growth inhibition on top and around some of the underlying streptococcal colonies. Fig. 6 shows

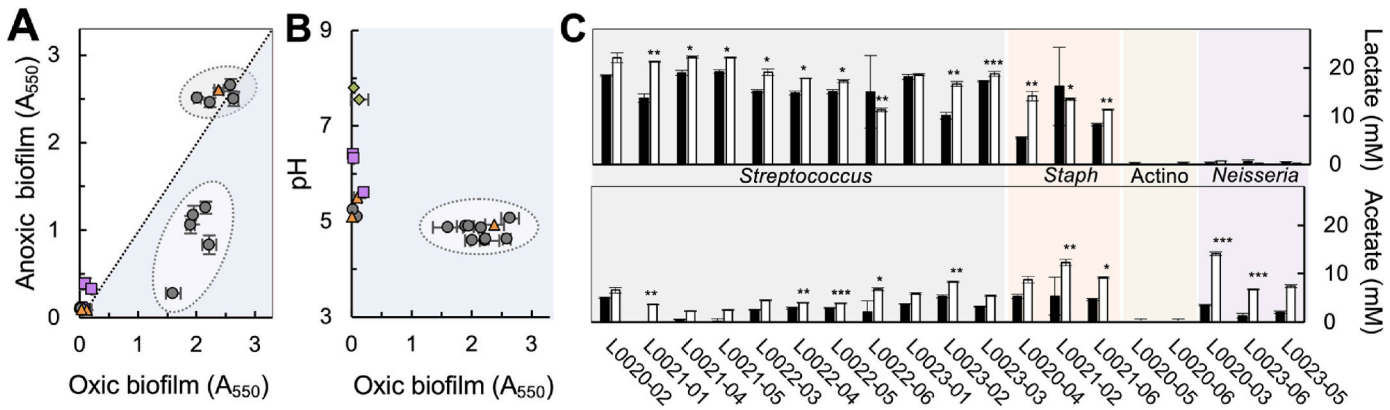

Fig. 5. Adaptive responses promoting the establishment of otic trophic webs. (**A**) Biofilm biomass (crystal violet staining, measured as absorbance at 550 nm, A_{550}) of otic isolates in oxic (blue) and anoxic (white) cultures. The dashed circles identify two separate clusters of isolates with highest biofilm-forming abilities. (**B**) Correlation between biofilm formation and pH in oxic cultures. The circle highlights a cluster of strains with highest biofilm-forming activities and lowest pH. (**C**) Lactate and acetate production (mM) in stationary-phase cultures grown in oxic (black) and anoxic (white) media. The asterisks show significant differences (*$p \leq 0.05$, **$p \leq 0.01$, ***$p \leq 0.001$) between oxic and anoxic values in a two-tailed *t*-test analysis with the Microsoft Excel® software. All data points in **A-C** are average values of three independent biological experiments and are color-coded for *Streptococcus* (gray), *Staphylococcus*(orange), *Neisseria* (purple) and actinobacterial genera *Micrococcus* and *Corynebacterium* (green). (For interpretation of the references to color in this figure legend, the reader is referred to the Web version of this article.)

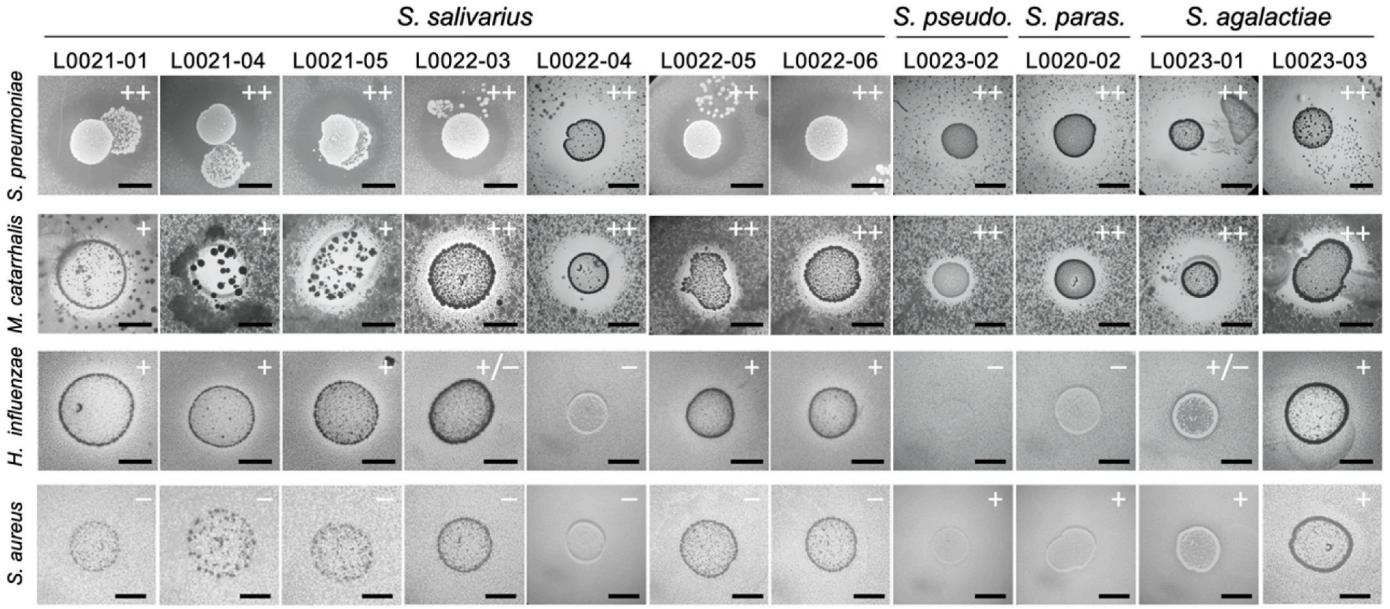

Fig. 6. Growth inhibition of common otopathogens by otic streptococci. TSA plates containing 24-h colonies of the otic streptococci were incubated for 24h with soft-agar overlays of the otopathogens *Streptococcus pneumoniae, Moraxella catarrhalis, Haemophilus influenzae* and *Staphylococcus aureus*. All incubations were at 37°C in atmospheric air. The plates show clear areas of growth inhibition of the otopathogen on top and/or around antagonistic streptococcal colonies underneath (scale bar, 0.5 cm). The symbols indicate average size of the growth inhibition halo around the underlying streptococcal colony in triplicate plate assays (+, <0.4; ++, >0.4; +/−, ~0.1 but not always reproducible).

representative plate assays for all the otic strains against each otopathogen and the zones of growth inhibition, which reveal antagonistic interactions due to nutrient competition, secretion of growth inhibitors by the streptococci, or both. The zones of growth inhibition are particularly large against *S. pneumoniae* and *M. catarrhalis*, consistent with the secretion of a diffusible inhibitory compound. By contrast, antagonistic effects against *H. influenzae* were less pronounced and strain-specific (Fig. 6).

We also used the plate assay to screen for potential antagonism of the otic streptococci towards the nasopharyngeal staphylococci. As a test strain, we used *S. aureus* subsp. *aureus* JE2 [22], a plasmid-cured derivative of the epidemic community-associated methicillin-resistant *S. aureus* (CA-MRSA) isolate USA300 [17]. We observed antagonism by all the non-Salivarius isolates (Fig. 6), indicative of a species-specific mechanism for growth inhibition by these streptococcal groups (*S. pseudopneumoniae*, *S. parasanguinis* and *S. agalactiae*). The ability of non-Salivarius streptococci to inhibit the growth of *S. aureus* is not uncommon. Despite being catalase positive, *S. aureus* is sensitive to hydrogen peroxide produced by *S. pneumoniae* in the nasal mucosa [61]. This is because hydrogen peroxide is converted into a highly toxic hydroxyl radical (•OH) that rapidly kills *S. aureus* [82]. However, non-Salivarius otic streptococci release hydrogen peroxide as a byproduct of their metabolism [19,59,80] and use catalase-independent mechanisms for anti-oxidative stress resistance [11]. These phenotypic traits confer on the streptococcal isolates a competitive advantage during the colonization of the middle ear mucosa and help explain why *Staphylococcus* sequences are seldom detected in otic secretions [44].

3. Discussion

The recovery from otic secretions of close relatives of oral bacteria (Fig. 2) highlights the role that saliva aerosols play in the dispersal of bacteria through the aerodigestive tract. Human saliva carries bacteria shed from oral surfaces such as teeth and gums and spreads them to distant mucosae [13,47]. The constant flux of saliva to the oropharynx (back of the throat) facilitates the formation of aerosols and oral bacterial carriage to the middle ear every time the Eustachian tube opens [44]. In support of this, phylogenetic analysis of full-length 16S rRNA sequences resolved close evolutionary relationships between the otic cultivars and species that reside or transiently disperse in the oral cavity (Fig. 2). Particularly important were the ancestral ties between the otic streptococci and pioneer species of oral biofilms. Most of the otic streptococci were closely related to *S. salivarius,* one of the first colonizers of the human oral cavity after birth and an abundant commensal throughout the life of the host [31]. This bacterium disperses as aggregates that survive stomach passage [26] and seed the mucosa of the small intestine [78]. *S. salivarius* aggregates may also disperse in saliva aerosols, a dispersal path that provides the primary mechanism for seeding of the otic mucosa [44]. Streptococcal aggregation could facilitate immunoescape and the formation of microcolonies on the otic mucosal epithelium. It may also promotes coaggregation with anaerobic syntrophic partners and support trophic interactions (Fig. 1) that mirror those described in oral biofilms. Additionally, oral *S. salivarius* strains mediate antagonistic interactions with virulent streptococci that prevent tooth decay, periodontal disease, and the spread of respiratory pathogens such as the otopathogen *S. pneumoniae* [74,75]. We observed similar interspecies interference of otic *S. salivarius* strains towards common otopathogens (Fig. 6), suggesting similar roles for these middle ear residents in disease prevention.

The non-Salivarius otic streptococci were also close relatives of oral species (Fig. 2). For example, one of the isolates (L0020-02) was closely related to *S. parasanguinis*, a bacterium that groups with species in the Mitis group based on 16S rRNA gene sequence analysis and that shares with them many phenotypic characteristics [21]. Like *S. salivarius*, *S. parasanguinis* is one of the early colonizers of the oral cavity [39] and disperses in saliva [77]. It produces fimbriae to firmly attach to and co-disperse within syntrophic oral aggregates [24]. The otic streptococci also included strains closely related to *S. pseudopneumoniae* (L0023-02; Viridans group) and *S. agalactiae* (L0023–01 and L0023-03; GBS group), which are oral streptococci linked to infective processes in the aerodigestive tract and other body sites [34,58]. Yet, the otic relatives readily inhibited the growth of the three most common otopathogens (*S. pneumoniae*, *M. catarrhalis*, and non-typeable *H. influenzae*) and were the only otic streptococci that interfered with the growth of *S. aureus* (Fig. 6). Antagonism towards *S. aureus* may involve the production of hydrogen peroxide as a metabolic byproduct, as noted for related oral streptococcal species [19,59,80]. Hydrogen peroxide also functions as a signaling molecule for the co-aggregation of non-salivarius streptococci in syntrophic biofilms [19]. Future studies will need to evaluate the role of these streptococcal lineages in producing hydrogen peroxide as a signal for intra and interspecies co-aggregation and as an antagonist of bacterial competitors in the middle ear mucosa.

The results presented in this study also identified physiological traits of streptococci that could facilitate the colonization of the middle ear mucosa and the formation of syntrophic biofilms. The otic streptococci were all temperate swarmers on soft agar plates (Fig. 3) and only some secreted surfactants (Table 2). Endogenous surfactants stimulate swarming on semisolid agar surfaces but may not be needed for efficient swarming through the native mucus layers [53]. This is particularly true for bacteria colonizing the middle ear mucosa, which is rich in host surfactants [49]. Furthermore, surfactant production by bacterial colonizers may be undesirable in the middle ear mucosa, as it could change the mucus rheology and interfere with critical mucosal functions such as antimicrobial activity, immunomodulation and Eustachian tube mechanics [49]. Indeed, careful control of host surfactants regulates the viscosity and surface tension of the tympanic mucus layer [25] and keeps the surface tension of the mucus sufficiently low (58 mN/m) to facilitate the opening of the collapsed Eustachian tube [49]. Disruption of surfactant homeostasis increases the pressure needed to open the Eustachian tube, risking barotrauma and making the middle ear mucosa more vulnerable to infections [49].

An important finding of our study was the identification of phenotypic traits in streptococcal and staphylococcal cultivars that could give both groups a competitive advantage during the colonization of the middle ear. For example, the streptococcal and staphylococcal isolates grew well with and without oxygen (Fig. 4A) and secreted mucins and proteases (Table 3), which are adaptive responses for growth and reproduction under otic redox fluctuations using the available mucosal nutrients. Moreover, both groups produced lactate as the main fermentation byproduct (Fig. 5C), a key metabolic intermediate in the syntrophic otic communities [44]. By contrast, the otic *Neisseria* strains L0020–05 and L0020-06 grew poorly and flocculated extensively in oxic broth (Fig. 4A). Furthermore, the strains did not form robust biofilms (Fig. 5A), nor did they produce lactate fermentatively (Fig. 5C). These two *Neisseria* species formed a separate clade with species in the family *Neisseriaceae* that populate the tongue dorsum [18]. And although these species readily disperse via saliva into the oropharynx [45], they are not positively selected in the middle ear [44]. Additionally, the *Neisseria* cultivars were, along with the actinobacterial isolates (*Micrococcus* spp. L0020-05 and *Corynebacterium* spp. L0020-06), the only strains that did not secrete proteases on casein plates (Table 3). Not surprisingly, despite their abundance in the oral and perioral regions [41], these groups are not enriched in otic secretions [44].

The most notable difference between the staphylococcal and streptococcal isolates was arguably the aggregative properties of most *Streptococcus* species (Fig. 3B). Aggregation allows oral streptococci to recognize and recruit other bacteria to biofilms [46]. For example, oral streptococci coaggregate with actinomyces to colonize the tooth surface and recruit other bacteria during the formation of the dental plaque [39,42]. Lactate exchange between streptococcal and *Veillonella* strains is critical for coaggregation during the early stages of biofilm formation on oral surfaces [46]. Fusobacteria also mediate early coaggregation in oral biofilms, forming physical bridges across the microcolonies that facilitate the attachment of non-coaggregating bacteria [39,42]. Thus, aggregative behaviors drive syntrophic interactions that sustain the growth of the dental plaque throughout all dentition stages and during the formation of subgingival biofilms in the predentate and postdentate states [47]. Being widespread and abundant, oral co-aggregates promote the co-dispersal of streptococci and syntrophic partners in saliva [3] and afford immunoprotection in non-oral mucosae [72].

The fact that the otic streptococci, like the oral ancestors, were highly aggregative (Fig. 4), formed robust biofilms (Fig. 5A) and produced lactate (Fig. 4C) suggests that they are the primary colonizers of the middle ear mucosa. These adaptive traits allow streptococci to grow and reproduce in the middle ear mucosa with obligate anaerobic, syntrophic partners such as *Prevotella, Fusobacterium* and *Veillonella* [44]. The syntrophic microcolonies metabolize and ferment host mucins and proteins in the otic mucosa (Fig. 1), indirectly controlling the viscoelastic properties of the mucus layer and Eustachian tube functionality [49]. The detection of a differential gradient of mucin gene expression along the tympanic cavity and Eustachian tube [49] suggests a high degree of spatial heterogeneity in bacterial colonization as well. Shaped like an inverted flask [6], the posterior region of the Eustachian tube is more readily seeded with saliva aerosols during the cycles of tubal aperture. Concentration of streptococcal aggregates in this region closer to the nasopharyngeal opening of the Eustachian tube could provide increased protection against otopathogens, which typically reside in nasal reservoirs. Future research should therefore consider the mechanisms that allow otic streptococci to co-aggregate with syntrophic partners, their spatial distribution in the otic mucosa and antagonistic

interactions with transient migrants. This knowledge is important to understand the functionality of the otic communities and how they influence host functions and the outcome of infections.

4. Methods

Bacterial strains and culture conditions. The bacterial strains used in this study include 19 cultivars previously isolated from otic secretions [44]. Briefly, the samples were collected with a single swab from the left and right nasopharyngeal openings of the Eustachian tube in 4 young (19–32 years old), healthy adults recruited as part of a larger study approved by the Michigan State University Biomedical and Physical Health Review Board (IRB # 17–502). All the strains were isolated as single colonies on Tryptic Soy Agar (TSA) plates (30 g/L of Tryptic Soy Broth from Sigma Aldrich and 15 g/L of Bacto Agar from BD) grown at 37°C. The isolates were routinely grown overnight in 5 ml of Tryptic Soy Broth (TSB) at 37°C with gentle agitation. For growth studies, we transferred mid-log phase (OD_{600} ~0.5) TSB cultures twice (initial OD_{600} of 0.1) to prepare a stationary phase (~0.9–1.0 OD_{600}) inoculum for growth assays in Corning® 96-well clear round bottom TC-treated microplates (Corning 3799). Growth was initiated with the addition of 18 μl of the inoculum to 162 μl of TSB per well and monitored spectrophotometrically every 30 min (OD_{630} readings after 0.1 s of gentle agitation) while incubating the plates at 37°C inside a PowerWave HT (BioTek) plate reader. Each microtiter plate contained a control well with TSB medium (no cells) to use as a blank. To test for growth in anoxic medium, we introduced the inoculated plates in an 855-ABC Portable Anaerobic Chamber (Plas Labs, Inc.) containing a headspace of N_2:CO_2 (80:20), removed the lid several times to disperse the air, and allowed the media to equilibrate in the anoxic atmosphere for 10 min. We then placed the plate in a plate reader (PowerWave HT, BioTek) housed inside the anaerobic chamber. Microplate OD readings were every 30 min after 0.1 s of agitation. We used the ANOVA (Analysis of Variance) test in the Microsoft Excel® software to determine the significance of the difference between the means of aerobic and anaerobic growth (generation times) for each taxonomic group.

DNA sequencing and phylogenetic analyses. For taxonomic and phylogenetic analyses, we grew the 19 otic isolates (Table 1) in 2 ml of TSB at 37°C for 24 h and harvested the cells by centrifugation (25,000×*g* for 5 min) in an Eppendorf 5417R refrigerated centrifuge prior to extracting the genomic DNA with a FastDNA™ Spin kit (MP Biomedicals). Library preparation with an Illumina Nextera kit and whole genome sequencing in an Illumina NextSeq 550 platform were at the Microbial Genome Sequencing Center (MiGS; Pittsburgh, PA). We used the FastQC tool from the Babraham Institute (https://www.bioinformatics.babraham.ac.uk/projects/fastqc/) for sequence quality control and Trimmomatics [7] for cleaning/trimming of the Illumina short reads. After assembling the genomes *de novo* with the Spades assembler [1], we identified the 16S rRNA gene sequences in the contigs with the BAsic Rapid Ribosomal RNA Predictor (Barnap) (https://github.com/tseemann/barrnap). The 16S rRNA gene sequences were deposited in the GenBank database under individual accession numbers (Table 1). We used these sequences to identify the closest species (% identity) in the GenBank database using the nucleotide Basic Local Alignment Search Tool (BLAST) at the U.S. National Center of Biological Information (NCBI) using an species identity cutoff value of 98.7% [70]. We retrieved the 16S rRNA gene sequences from the closest type strains listed in the SILVA rRNA database (https://www.arb-silva.de) and aligned them to the otic sequences with the MUSCLE program using the MEGA X software [43]. We used the alignment to build a maximum-likelihood phylogenetic tree and calculate bootstrap confidence values for each node using 1,000 replications. The tree shows bootstrap values above 50% [27].

Catalase assay. Frozen stocks of the otic isolates were directly streaked on 1.5% (w/v) TSA plates to grow individual colonies at 37°C overnight. We spread each colony onto a microscope slide and added a drop of freshly prepared 3% hydrogen peroxide. Catalase-positive strains break down the hydrogen peroxide into water and oxygen gas, which generates bubbles. Lack or weak production of bubbles was used to designate a strain as catalase negative.

Swarming motility and surfactant detection assays. We screened each otic isolate for their ability to move on soft (0.5% and, when indicated, 0.4% w/v agar) TSA plates, as a modification of a previously described assay [57]. For these assays, we first grew each isolate and the positive control (*P. aeruginosa* PA01) in TSB at 37°C overnight (OD_{600} ~1) and prepared a diluted TSB inoculum (OD_{600} 0.1). We pipetted a 5-μl drop of the diluted culture onto the surface of the soft agar plates and allowed it to absorb until completely dry (~30 min). We then incubated the plates at 37°C and photographed the areas of growth at 18, 42 and 62 h against a ruler using a dissecting scope (Leica MZ6) at a magnification of 0.8X and 1X. The photographs were then analyzed with the ImageJ software [66] to measure the colony diameter over time and calculate the area expansion (swarming distance) from the initial inoculation spot.

We also screened the ability of the otic isolates to produce surfactants with a previously described atomized oil assay [10]. For this, we plated a 5-μl drop of the diluted TSB culture (OD_{600} of 0.1) on agar-solidified (1.5% w/v) TSA medium, allowed the inoculum to absorb for ~30 min, and incubated the plates at 37°C for 24 h. Using an airbrush (type H; Paasche Airbrush Co., Chicago, IL), we applied a fine mist of mineral oil onto the plate surface. Surfactant-producing colonies readily display a halo of mineral oil dispersal whose size provides a semiquantitative measure of surfactant secretion [10]. Photography and halo diameter visualization were as described above for the swarming assays, except that we measured the size of the oil dispersal zone from the colony edge. All strains were tested in three independent swarming and surfactant assays plates to calculate the average and standard deviation values.

Protease and mucinase plate assays. We used TSA plates containing 5% lactose-free, skim milk (Fairlife, LLC) or 0.5% Type II porcine gastric mucin (Sigma Aldrich) to screen the otic isolates for mucinase and protease secretion, respectively, using *P. aeruginosa* PA01 as a positive control. For these assays, we spot-plated 5 μl of overnight TSB cultures and incubated at 37°C for 24 h, as described earlier for the surfactant assays. Strains that secrete proteases to the medium degrade the milk's casein and produce a clear halo around the area of growth after 24 h of incubation. Mucinase producers have clearings (mucin lysis) around or under the colony that show as zones of discoloration after staining with 7 ml of 0.1% amido black for 30 min and destaining with 14 ml of 2.5 M acetic acid for 30 min. When indicated, plates were incubated for 48 h to confirm emerging phenotypes. Each strain was tested in triplicate and photographed on a lightboard (A4 LED Light Box 9x12 Inch Light Pad, ME456) with an iPhone 11 at 2.4x magnification.

Organic acid detection in culture supernatant fluids. We grew triplicate stationary phase cultures of the otic isolates in oxic and anoxic TSB medium at 37°C and harvested the culture supernatant fluids by centrifugation (14,000 rpm, 10 min). We measured the pH of the supernatant fluids (5 ml) with a pH probe (Thermo Scientific™ Orion™ 720A + benchtop pH meter) and stored 1 ml of the samples at −20°C for chemical analyses by high performance liquid chromatography (HPLC). Once thawed, we filter-sterilized 250 μl of the supernatant fluid into 1-ml HPLC vials and measured their organic acid content in a Shimadzu 20A HPLC equipped with an Aminex HPX-87H column and a Micro-Guard cation H^+ guard column (Bio-Rad, Hercules, CA) at 55°C, as previously described [20]. As controls, we included samples with TSB medium and standard solutions of acetate, lactate, and pyruvate (provided at 1, 2, 5, 10 or 20 mM).

Biofilm assays. We used a previously described assay [50] to test the ability of the otic cultivars to form biofilms in Corning® 96-well clear round bottom TC-treated microplates (Corning 3799). We first grew overnight cultures in TSB with gentle agitation (~200 rpm) and used them to prepare a diluted cell suspension (OD_{600} ~0.1) for inoculation (18 μl) into TSB medium (162 μl per well). Each isolate was tested in 8

replicate wells. After incubating the plates at 37°C for 24 h, we removed the planktonic culture, washed the wells with ddH_2O and stained the surface-attached cells with 0.1% (w/v) crystal violet. We then rinsed the wells with water and let the stained biofilms to dry overnight at room temperature before solubilizing the biofilm-associated crystal violet with 180 μl of 30% glacial acetic acid and measuring the crystal violet in the solution spectrophotometrically at 550 nm [50]. Correlations between aerobic biofilm formation and culture acidification were statistically analyzed and visualized with the K-mean clustering R functions (https://www.rdocumentation.org/packages/stats/versions/3.6.2/topics/kmeans) available in the RStudio software (version 4.0.4). Clustering visualization in R-Studio was achieved by plotting k-mean cluster results against desired averaged datasets (oxic-anoxic biofilm formation, aerobic pH, or aerobic doubling time).

Growth inhibition plate assays. We screened the otic streptococcal isolates for their ability to inhibit the growth of bacterial species (*S. pneumoniae, M. catarrhalis,* and non-typeable *H influenzae*) commonly associated with infections of the middle ear [64]. As test strains, we used *S. pneumoniae* ATCC 6303 and *M. catarrhalis* ATCC 25238 (from the laboratory strain collection of Dr. Martha Mulks, Department of Microbiology and Molecular Genetics, Michigan State University) and a non-typeable *H. influenzae* (NTHi) strain isolated by Dr. Poorna Viswanathan in the teaching lab of the Department of Microbiology and Molecular Genetics (Michigan State University). The NTHi strain was confirmed prior to experimental use by multiplex PCR confirmation, as described previously [81]. We also included for testing the laboratory strain *S. aureus* JE2, which was kindly provided by Dr. Neal Hammer (Department of Microbiology and Molecular Genetics, Michigan State University). The otic streptococci and *S. aureus* JE2 were routinely grown in 5 ml TSB at 37°C with gentle agitation to prepare overnight cultures for the plate assays. *S. pneumoniae* and *M. catarrhalis* were grown at 37°C overnight in 5 mL of brain heart infusion (BHI) broth (Sigma-Aldrich) without agitation. The NTHi reference strain of *H. influenzae* was also grown statically at 37°C but in supplemented BHI (sBHI) [55], which contains (per L): 30 g BHI, 0.01 mg hemin (Bovine, Sigma Aldrich), and 0.002 mg β-Nicotinamide adenine dinucleotide sodium salt (Sigma Aldrich). All incubations were in a 37°C incubator with a 5% CO_2 atmosphere except for *S. aureus*, which were in air.

We used the spot-on-lawn method [65] to investigate antagonistic interactions between the otic streptococci and test strains. We first spotted 5 μl of a diluted (OD_{600} of 0.1) overnight culture of each streptococcal strain onto a 1.5% (w/v agar) TSA plate and allowed it to dry for 30 min at room temperature before incubating at 37°C for 24 h to grow the colonies. We then overlayed the plates with a warm (55°C) 8-ml layer of soft-agar (0.75%, w/v, final concentration) medium (TSA, BHI or sBHI) containing the test strain (OD_{600} of 0.1). The general procedure to make 0.75% agar overlays was to autoclave 6 ml of 1% agar-solidified growth medium, cool down the melted agar in a 55°C water bath, add 2 ml of the test strain culture to a final OD_{600} of 0.1, and mix by inversion before pouring over the TSA plate surface with the otic colonies. To make sBHI overlays, we added the chemical supplements to 6 ml of warm (55°C), melted 1% (w/v) agar BHI before mixing with 2 ml of an overnight NTHi culture to a final OD_{600} of 0.1. The overlays were allowed to solidify at room temperature before incubating for an additional 24 h at 37°C in an incubator with or without (*S. aureus* overlay) 5% CO_2. These culture conditions promoted the growth of the test strains as a turbid lawn in the overlays after 24 h, except for areas of growth inhibition (halos or clear zones) on top and around colonies of antagonistic streptococci growing underneath. At the end of the incubation period, we photographed the overlayed plates with a dissecting scope (0.63x objective) against a ruler and used the ImageJ program (4) to measure the size of the growth inhibition zone from the streptococcal colony edge underneath in triplicate biological replicates.

Availability of data and materials

The 16S rRNA gene sequences retrieved from Illumina sequences were deposited in the GenBank database under individual accession numbers (Table 1).

Ethics approval and consent to participate

The isolates used in this study were originally recovered from human mucosal samples using a protocol approved on May 17 of 2017 by the Institutional Review Board (IRB) at Michigan State University, East Lansing, Michigan, United States of America. The committee found the research project to be appropriate in design, to protect the rights and welfare of human subjects, and to meet the requirements of Michigan State University's Federal Wide Assurance and the Federal Guidelines (45 CFR 46 and 21 CFR Part 50).

Consent for publication

Not applicable.

Funding

This research was funded by grants N00014-17-2678 and N00014-20-1-2471 from the Office of Naval Research (ONR) to GR. KJ acknowledges support from a summer 2020 G. D. Edith Hsiung and Margaret Everett Kimball Endowed fellowship from the department of Microbiology and Molecular Genetics at Michigan State University. The funders had no role in study design, data collection and analysis, decision to publish or preparation of manuscript.

CRediT authorship contribution statement

Kristin M. Jacob: Formal analysis, processed samples for cultivation experiments, sequenced and partially assembled the genomes of otic cultivars to retrieve 16S rRNA sequences, performed the taxonomic and phylogenetic analyses and all the physiological characterization assays. All authors read and approved the final version of the manuscript. **Gemma Reguera:** conceived the study and planned and interpreted the experiments with KJ, Writing – original draft, wrote the first draft of the manuscript and incorporated contributions from KJ. All authors read and approved the final version of the manuscript.

Declaration of competing interest

The authors declare the following financial interests/personal relationships which may be considered as potential competing interests: Gemma Reguera reports financial support was provided by Office of Naval Research. Kristin J Jacob reports a relationship with Michigan Department of Health and Human Services that includes: non-financial support.

Acknowledgements

The authors would like to thank Dr. Michaela TerAvest and Nicholas Tefft at Michigan State University for assistance with the HPLC analyses and Drs. Batsirai Mabvakure and Heather Blankenship at the Michigan Department of Health and Human Services Bureau of Laboratory for guidance on Illumina short read assembly and contig gene analysis. We are also thankful to Drs. Martha Mulks, Poorna Viswanathan and Neal Hammer for providing the test strains used in the growth inhibition plate assays.

References

[1] Bankevich A, Nurk S, Antipov D, Gurevich AA, Dvorkin M, Kulikov AS, et al. SPAdes: a new genome assembly algorithm and its applications to single-cell sequencing. J Comput Biol 2012;19(5):455–77. https://doi.org/10.1089/cmb.2012.0021.

[2] Bassis CM, Erb-Downward JR, Dickson RP, Freeman CM, Schmidt TM, Young VB, et al. Analysis of the upper respiratory tract microbiotas as the source of the lung and gastric microbiotas in healthy individuals. mBio 2015;6(2):e00037. https://doi.org/10.1128/mBio.00037-15. 00015.

[3] Belstrom D. The salivary microbiota in health and disease. J Oral Microbiol 2020;12(1):1723975. https://doi.org/10.1080/20002297.2020.1723975.

[4] Bible AN, Khalsa-Moyers GK, Mukherjee T, Green CS, Mishra P, Purcell A, et al. Metabolic adaptations of *Azospirillum brasilense* to oxygen stress by cell-to-cell clumping and flocculation. Appl Environ Microbiol 2015;81(24):8346–57. https://doi.org/10.1128/aem.02782-15.

[5] Blaak EE, Canfora EE, Theis S, Frost G, Groen AK, Mithieux G, et al. Short chain fatty acids in human gut and metabolic health. Benef Microbes 2020;11(5):411–55. https://doi.org/10.3920/BM2020.0057.

[6] Bluestone CD. The Eustachian Tube: structure, function, and role in the middle ear. Hamilton, Ontario: BC Decker Inc; 2005.

[7] Bolger AM, Lohse M, Usadel B. Trimmomatic: a flexible trimmer for Illumina sequence data. Bioinformatics 2014;30(15):2114–20. https://doi.org/10.1093/bioinformatics/btu170.

[8] Bomar L, Brugger SD, Lemon KP. Bacterial microbiota of the nasal passages across the span of human life. Curr Opin Microbiol 2018;41:8–14. https://doi.org/10.1016/j.mib.2017.10.023.

[9] Brugger SD, Bomar L, Lemon KP. Commensal–pathogen interactions along the human nasal passages. PLoS Pathog 2016;12(7):e1005633. https://doi.org/10.1371/journal.ppat.1005633.

[10] Burch AY, Shimada BK, Browne PJ, Lindow SE. Novel high-throughput detection method to assess bacterial surfactant production. Appl Environ Microbiol 2010;76(16):5363–72. https://doi.org/10.1128/AEM.00592-10.

[11] Chen Z, Wang X, Yang F, Hu Q, Tong H, Dong X. Molecular insights into hydrogen peroxide-sensing mechanism of the metalloregulator MntR in controlling bacterial resistance to oxidative stresses. J Biol Chem 2017;292(13):5519–31. https://doi.org/10.1074/jbc.M116.764126.

[12] Cotter PD, Hill C. Surviving the acid test: responses of gram-positive bacteria to low pH. Microbiol Mol Biol Rev 2003;67(3):429–53. https://doi.org/10.1128/mmbr.67.3.429-453.2003.

[13] Crielaard W, Zaura E, Schuller AA, Huse SM, Montijn RC, Keijser BJ. Exploring the oral microbiota of children at various developmental stages of their dentition in the relation to their oral health. BMC Med Genom 2011;4:22. https://doi.org/10.1186/1755-8794-4-22.

[14] Delorme C, Abraham AL, Renault P, Guédon E. Genomics of *Streptococcus salivarius*, a major human commensal. Infect Genet Evol 2015;33:381–92. https://doi.org/10.1016/j.meegid.2014.10.001.

[15] Delwiche EA, Pestka JJ, Tortorello ML. The *Veillonellae*: gram-negative cocci with a unique physiology. Annu Rev Microbiol 1985;39:175–93. https://doi.org/10.1146/annurev.mi.39.100185.001135.

[16] Dewhirst FE, Chen T, Izard J, Paster BJ, Tanner AC, Yu WH, et al. The human oral microbiome. J Bacteriol 2010;192(19):5002–17. https://doi.org/10.1128/JB.00542-10.

[17] Diep BA, Gill SR, Chang RF, Phan TH, Chen JH, Davidson MG, et al. Complete genome sequence of USA300, an epidemic clone of community-acquired meticillin-resistant *Staphylococcus aureus*. Lancet 2006;367(9512):731–9. https://doi.org/10.1016/s0140-6736(06)68231-7.

[18] Donati C, Zolfo M, Albanese D, Tin Truong D, Asnicar F, Iebba V, et al. Uncovering oral *Neisseria* tropism and persistence using metagenomic sequencing. Nature Microbiol 2016;1(7):16070. https://doi.org/10.1038/nmicrobiol.2016.70.

[19] Duan D, Scoffield JA, Zhou X, Wu H. Fine-tuned production of hydrogen peroxide promotes biofilm formation of *Streptococcus parasanguinis* by a pathogenic cohabitant *Aggregatibacter actinomycetemcomitans*. Environ Microbiol 2016;18(11):4023–36. https://doi.org/10.1111/1462-2920.13425.

[20] Duhl KL, Tefft NM, TerAvest MA. *Shewanella oneidensis* MR-1 utilizes both sodium- and proton-pumping NADH dehydrogenases during aerobic growth. Appl Environ Microbiol 2018;84(12):e00415. https://doi.org/10.1128/aem.00415-18. 00418.

[21] Facklam R. What happened to the streptococci: overview of taxonomic and nomenclature changes. Clin Microbiol Rev 2002;15(4):613. https://doi.org/10.1128/Cmr.15.4.613-630.2002.

[22] Fey PD, Endres JL, Yajjala VK, Widhelm TJ, Boissy RJ, Bose JL, et al. A genetic resource for rapid and comprehensive phenotype screening of nonessential *Staphylococcus aureus* genes. mBio 2013;4(1):e00537. https://doi.org/10.1128/mBio.00537-12. 00512.

[23] Gao L, Xu T, Huang G, Jiang S, Gu Y, Chen F. Oral microbiomes: more and more importance in oral cavity and whole body. Protein Cell 2018;9(5):488–500. https://doi.org/10.1007/s13238-018-0548-1.

[24] Garnett JA, Simpson PJ, Taylor J, Benjamin SV, Tagliaferri C, Cota E, et al. Structural insight into the role of Streptococcus parasanguinis Fap1 within oral biofilm formation. Biochem Biophys Res Commun 2012;417(1):421–6. https://doi.org/10.1016/j.bbrc.2011.11.131.

[25] Ghadiali SN, Banks J, Swarts JD. Effect of surface tension and surfactant administration on Eustachian tube mechanics. J Appl Phys 2002;93(3):1007–14. https://doi.org/10.1152/japplphysiol.01123.2001.

[26] Hakalehto E, Vilpponen-Salmela T, Kinnunen K, von Wright A. Lactic acid bacteria enriched from human gastric biopsies. ISRN Gastroenterol 2011:109183. https://doi.org/10.5402/2011/109183. 2011.

[27] Hall BG. Phylogenetic trees made easy: a how-to manual. fifth ed. New York: Sinauer Associates is imprint of Oxford University Press; 2018.

[28] Hall-Stoodley L, Hu FZ, Gieseke A, Nistico L, Nguyen D, Hayes J, et al. Direct detection of bacterial biofilms on the middle-ear mucosa of children with chronic otitis media. JAMA 2006;296(2):202–11. https://doi.org/10.1001/jama.296.2.202.

[29] Honjo I, Hayashi M, Ito S, Takahashi H. Pumping and clearance function of the eustachian tube. Am J Otolaryngol 1985;6(3):241–4. https://doi.org/10.1016/S0196-0709(85)80095-8.

[30] Huch M, De Bruyne K, Cleenwerck I, Bub A, Cho GS, Watzl B, et al. *Streptococcus rubneri* sp. nov., isolated from the human throat. Int J Syst Evol Microbiol 2013;63(Pt 11):4026–32. https://doi.org/10.1099/ijs.0.048538-0.

[31] Kaci G, Goudercourt D, Dennin V, Pot B, Doré J, Ehrlich SD, et al. Anti-Inflammatory properties of *Streptococcus salivarius*, a commensal bacterium of the oral cavity and digestive tract. Appl Environ Microbiol 2014;80(3):928–34. https://doi.org/10.1128/aem.03133-13.

[32] Kaito C, Sekimizu K. Colony spreading in *Staphylococcus aureus*. J Bacteriol 2007;189(6):2553–7. https://doi.org/10.1128/jb.01635-06.

[33] Kandler O. Carbohydrate metabolism in lactic acid bacteria. Antonie Leeuwenhoek 1983;49(3):209–24. https://doi.org/10.1007/bf00399499.

[34] Keith ER, Podmore RG, Anderson TP, Murdoch DR. Characteristics of *Streptococcus pseudopneumoniae* isolated from purulent sputum samples. J Clin Microbiol 2006;44(3):923–7. https://doi.org/10.1128/jcm.44.3.923-927.2006.

[35] Khan R, Petersen FC, Shekhar S. Commensal bacteria: an emerging player in defense against respiratory pathogens. Front Immunol 2019;10(1203). https://doi.org/10.3389/fimmu.2019.01203.

[36] Knapp JS, Hook 3rd EW. Prevalence and persistence of N*eisseria cinerea* and other *Neisseria* spp. in adults. J Clin Microbiol 1988;26(5):896–900. https://doi.org/10.1128/JCM.26.5.896-900.1988.

[37] Kocur M, Kloos WE, Schleifer K-H. The genus Micrococcus. In: Dworkin M, Falkow S, Rosenberg E, Schleifer K-H, Stackebrandt E, editors. The prokaryotes: volume 3: archaea. Bacteria: Firmicutes, actinomycetes. Springer New York, New York, NY; 2006. p. 961–71. https://doi.org/10.1007/0-387-30743-5_37.

[38] Köhler T, Curty LK, Barja F, van Delden C, Pechère J-C. Swarming of *Pseudomonas aeruginosa* Is dependent on cell-to-cell signaling and requires flagella and pili. J Bacteriol 2000;182(21):5990–6. https://doi.org/10.1128/jb.182.21.5990-5996.2000.

[39] Kolenbrander PE. Oral microbial communities: biofilms, interactions, and genetic systems. Annu Rev Microbiol 2000;54:413–37. https://doi.org/10.1146/annurev.micro.54.1.413.

[40] Kooken JM, Fox KF, Fox A. Characterization of *Micrococcus* strains isolated from indoor air. Mol Cell Probes 2012;26(1):1–5. https://doi.org/10.1016/j.mcp.2011.09.003.

[41] Koskinen K, Reichert JL, Hoier S, Schachenreiter J, Duller S, Moissl-Eichinger C, et al. The nasal microbiome mirrors and potentially shapes olfactory function. Sci Rep 2018;8(1):1296. https://doi.org/10.1038/s41598-018-19438-3.

[42] Kriebel K, Hieke C, Müller-Hilke B, Nakata M, Kreikemeyer B. Oral biofilms from symbiotic to pathogenic interactions and associated disease –Connection of periodontitis and rheumatic arthritis by peptidylarginine deiminase. Front Microbiol 2018;9(53). https://doi.org/10.3389/fmicb.2018.00053.

[43] Kumar S, Stecher G, Li M, Knyaz C, Tamura K. MEGA X: molecular evolutionary Genetics analysis across computing platforms. Mol Biol Evol 2018;35(6):1547–9. https://doi.org/10.1093/molbev/msy096.

[44] Lee J-Y, Jacob KM, Kashefi K, Reguera G. Oral seeding and niche-adaptation of middle ear biofilms in health. Biofilms 2021;3:100041. https://doi.org/10.1016/j.bioflm.2020.100041.

[45] Liu G, Tang CM, Exley RM. Non-pathogenic *Neisseria*: members of an abundant, multi-habitat, diverse genus. Microbiology 2015;161(7):1297–312. https://doi.org/10.1099/mic.0.000086.

[46] Mashima I, Nakazawa F. Interaction between *Streptococcus* spp. and *Veillonella tobetsuensis* in the early stages of oral biofilm formation. J Bacteriol 2015;197(13):2104–11. https://doi.org/10.1128/jb.02512-14.

[47] Mason MR, Chambers S, Dabdoub SM, Thikkurissy S, Kumar PS. Characterizing oral microbial communities across dentition states and colonization niches. Microbiome 2018;6(1):67. https://doi.org/10.1186/s40168-018-0443-2.

[48] McCormack MG, Smith AJ, Akram AN, Jackson M, Robertson D, Edwards G. *Staphylococcus aureus* and the oral cavity: an overlooked source of carriage and infection? Am J Infect Control 2015;43(1):35–7. https://doi.org/10.1016/j.ajic.2014.09.015.

[49] McGuire JF. Surfactant in the middle ear and eustachian tube: a review. Int J Pediatr Otorhinolaryngol 2002;66(1):1–15. https://doi.org/10.1016/s0165-5876(02)00203-3.

[50] Merritt JH, Kadouri DE, O'Toole GA. Growing and analyzing static biofilms. Current. Protocol. Microbiol. 2005. https://doi.org/10.1002/9780471729259.mc01b01s00 [Chapter 1]:Unit 1B 1.

[51] Munoz R, Yarza P, Ludwig W, Euzeby J, Amann R, Schleifer KH, et al. Release LTPs104 of the all-species living tree. Syst Appl Microbiol 2011;34(3):169–70. https://doi.org/10.1016/j.syapm.2011.03.001.

[52] Ohara-Nemoto Y, Haraga H, Kimura S, Nemoto TK. Occurrence of staphylococci in the oral cavities of healthy adults and nasal oral trafficking of the bacteria. J Med Microbiol 2008;57(Pt 1):95–9. https://doi.org/10.1099/jmm.0.47561-0.

[53] Partridge JD, Harshey RM. Swarming: flexible roaming plans. J Bacteriol 2013;195(5):909–18. https://doi.org/10.1128/jb.02063-12.

[54] Patterson MJ. Streptococcus. In: Baron S, editor. Medical microbiology. fourth ed. 1996. Galveston (TX).
[55] Poje G, Redfield RJ. General methods for culturing *Haemophilus influenzae*. Methods Mol Med 2003;71:51–6. https://doi.org/10.1385/1-59259-321-6:51.
[56] Pollitt EJG, Diggle SP. Defining motility in the *staphylococci*. Cell Mol Life Sci 2017; 74(16):2943–58. https://doi.org/10.1007/s00018-017-2507-z.
[57] Quinones B, Dulla G, Lindow SE. Quorum sensing regulates exopolysaccharide production, motility, and virulence in *Pseudomonas syringae*. Mol Plant Microbe Interact 2005;18(7):682–93. https://doi.org/10.1094/MPMI-18-0682.
[58] Raabe VN, Shane AL. Group B Streptococcus (*Streptococcus agalactiae*). Microbiol Spectr 2019;7(2). https://doi.org/10.1128/microbiolspec.GPP3-0007-2018. 10.1128/microbiolspec.GPP1123-0007-2018.
[59] Redanz S, Cheng X, Giacaman RA, Pfeifer CS, Merritt J, Kreth J. Live and let die: hydrogen peroxide production by the commensal flora and its role in maintaining a symbiotic microbiome. Mol Oral Microbiol 2018;33(5):337–52. https://doi.org/10.1111/omi.12231.
[60] Reddy MS, Murphy TF, Faden HS, Bernstein JM. Middle ear mucin glycoprotein: purification and interaction with nontypable *Haemophilus influenzae* and *Moraxella catarrhalis*. Otolaryngol Head Neck Surg 1997;116(2):175–80. https://doi.org/10.1016/S0194-59989770321-8.
[61] Regev-Yochay G, Trzcinski K, Thompson CM, Malley R, Lipsitch M. Interference between *Streptococcus pneumoniae* and *Staphylococcus aureus*: in vitro hydrogen peroxide-mediated killing by *Streptococcus pneumoniae*. J Bacteriol 2006;188(13): 4996–5001. https://doi.org/10.1128/JB.00317-06.
[62] Rios-Covian D, Salazar N, Gueimonde M, de los Reyes-Gavilan CG. Shaping the metabolism of intestinal *Bacteroides* population through diet to improve human health. Front Microbiol 2017;8. https://doi.org/10.3389/fmicb.2017.00376.
[63] Sade J. Mucociliary flow in the middle ear. Ann Otol Rhinol Laryngol 1971;80(3): 336–41. https://doi.org/10.1177/000348947108000306.
[64] Schilder AG, Chonmaitree T, Cripps AW, Rosenfeld RM, Casselbrant ML, Haggard MP, et al. Otitis media. Nat Rev Dis Prim 2016;2(1):16063. https://doi.org/10.1038/nrdp.2016.63.
[65] Schillinger U, Lücke FK. Antibacterial activity of *Lactobacillus* sake isolated from meat. Appl Environ Microbiol 1989;55(8):1901–6. https://doi.org/10.1128/aem.55.8.1901-1906.1989.
[66] Schneider CA, Rasband WS, Eliceiri KW. NIH Image to ImageJ: 25 years of image analysis. Nat Methods 2012;9(7):671–5. https://doi.org/10.1038/nmeth.2089.
[67] Sheng J, Marquis RE. Enhanced acid resistance of oral streptococci at lethal pH values associated with acid-tolerant catabolism and with ATP synthase activity. FEMS Microbiol Lett 2006;262(1):93–8. https://doi.org/10.1111/j.1574-6968.2006.00374.x.
[68] Siegel SJ, Weiser JN. Mechanisms of bacterial colonization of the respiratory tract. Annu Rev Microbiol 2015;69:425–44. https://doi.org/10.1146/annurev-micro-091014-104209.
[69] Smith PA, Sherman JM. The lactic acid fermentation of streptococci. J Bacteriol 1942;43(6):725–31. https://doi.org/10.1128/JB.43.6.725-731.1942.
[70] Stackebrandt E, Ebers J. Taxonomic parameters revisited: tarnished gold standards. Microbiol Today 2006;33(4):152–5.
[71] Tonnaer EL, Mylanus EA, Mulder JJ, Curfs JH. Detection of bacteria in healthy middle ears during cochlear implantation. Arch Otolaryngol Head Neck Surg 2009; 135(3):232–7. https://doi.org/10.1001/archoto.2008.556.
[72] Trunk T, Khalil HS, Leo JC. Bacterial autoaggregation. AIMS Microbiol 2018;4(1): 140–64. https://doi.org/10.3934/microbiol.2018.1.140.
[73] Tsompanidou E, Denham EL, Becher D, de Jong A, Buist G, van Oosten M, et al. Distinct roles of phenol-soluble modulins in spreading of *Staphylococcus aureus* on wet surfaces. Appl Environ Microbiol 2013;79(3):886–95. https://doi.org/10.1128/aem.03157-12.
[74] Van Hoogmoed CG, Geertsema-doornbusch GI, Teughels W, Quirynen M, Busscher HJ, Van der Mei HC. Reduction of periodontal pathogens adhesion by antagonistic strains. Oral Microbiol Immunol 2008;23(1):43–8. https://doi.org/10.1111/j.1399-302X.2007.00388.x.
[75] Van Hoogmoed CG, Geertsema-Doornbusch GI, Teughels W, Quirynen M, Busscher HJ, Van der Mei HC. Reduction of periodontal pathogens adhesion by antagonistic strains. Oral Microbiol Immunol 2008;23(1):43–8. https://doi.org/10.1111/j.1399-302X.2007.00388.x.
[76] Wandersman C. Secretion, processing and activation of bacterial extracellular proteases. Mol Microbiol 1989;3(12):1825–31. https://doi.org/10.1111/j.1365-2958.1989.tb00169.x.
[77] Wang K, Lu W, Tu Q, Ge Y, He J, Zhou Y, et al. Preliminary analysis of salivary microbiome and their potential roles in oral lichen planus. Sci Rep 2016;6:22943. https://doi.org/10.1038/srep22943.
[78] Wang M, Ahrné S, Jeppsson B, Molin G. Comparison of bacterial diversity along the human intestinal tract by direct cloning and sequencing of 16S rRNA genes. FEMS Microbiol Ecol 2005;54(2):219–31. https://doi.org/10.1016/j.femsec.2005.03.012.
[79] Welch JLM, Dewhirst FE, Borisy GG. Biogeography of the oral microbiome: the site-specialist hypothesis. Annu Rev Microbiol 2019. https://doi.org/10.1146/annurev-micro-090817-062503.
[80] Wilson CB, Weaver WM. Comparative susceptibility of group B streptococci and *Staphylococcus aureus* to killing by oxygen metabolites. J Infect Dis 1985;152(2): 323–9. https://doi.org/10.1093/infdis/152.2.323.
[81] World Health O, Centers for Disease C, Prevention. Laboratory methods for the diagnosis of meningitis caused by *Neisseria meningitidis, Streptococcus pneumoniae,* and *Haemophilus influenzae*: WHO manual. second ed. edn. Geneva: World Health Organization; 2011.
[82] Wu X, Gordon O, Jiang W, Antezana BS, Angulo-Zamudio UA, Del Rio C, et al. Interaction between *Streptococcus pneumoniae* and *Staphylococcus aureus* generates OH radicals that rapidly kill *Staphylococcus aureus* strains. J Bacteriol 2019;201 (21). https://doi.org/10.1128/jb.00474-19.
[83] Yarza P, Richter M, Peplies J, Euzeby J, Amann R, Schleifer KH, et al. The All-Species Living Tree project: a 16S rRNA-based phylogenetic tree of all sequenced type strains. Syst Appl Microbiol 2008;31(4):241–50. https://doi.org/10.1016/j.syapm.2008.07.001.
[84] Zhao G-Z, Li J, Qin S, Zhang Y-Q, Zhu W-Y, Jiang C-L, et al. *Micrococcus yunnanensis* sp. nov., a novel actinobacterium isolated from surface-sterilized *Polyspora axillaris* roots. Int J Syst Evol Microbiol 2009;59(10):2383–7. https://doi.org/10.1099/ijs.0.010256-0.